9 Helium Charge Exchange in Cometary Atmospheres

In this chapter we will focus on the interaction of helium ions from the solar wind with molecules that are abundant in cometary and planetary atmospheres. In Chapter 5 state selective cross sections for collisions between helium ions and H_2O, CO_2, CO and CH_4 were presented. From the laboratory results we deduce data sets for EUV emission in astrophysical environments. These cross sections are the ingredients in our model calculations of cometary helium emission. Using these spectra, we show in Section 9.3 how EUV emission can be analyzed in terms of solar wind and comet characteristics and apply this to existing observations of the comets C/1996 B2 (Hyakutake) and C/1995 O1 (Hale-Bopp).

9.1 Model Results

The sensitivity of charge exchange processes to properties of both the solar wind and the comet leads to many observable effects. The observation of helium emission from comets can therefore be used to probe the characteristics of the comet – solar wind interaction.

In this chapter, we shall use comet Halley as our standard case and adopt the comet and solar wind characteristics that were observed during the *Giotto* encounter, i.e. a gas production of 7×10^{29} molecules s^{-1} of which 10% CO molecules, located at 1 AU from the Sun and encountering a solar wind with $v(\infty)$ = 370 km s^{-1}, $n_p(\infty)$ = 10 cm^{-3} and a solar wind alpha abundace of 2% (Fuselier et al., 1991).

9.1.1 Intensities

Changing the cometary and/or solar wind parameters affects the absolute and relative emission line intensities. This is illustrated in Fig. 9.1, where the total luminosity of the HeII 30.4 nm is plotted against the total luminosity of the HeI 58.4 nm line for a Halley-like interaction. The luminosity of the HeII 30.4 nm line increases by four orders of magnitude as the velocity increases from 100 to 1000 km s^{-1}, whereas the luminosity of the HeI

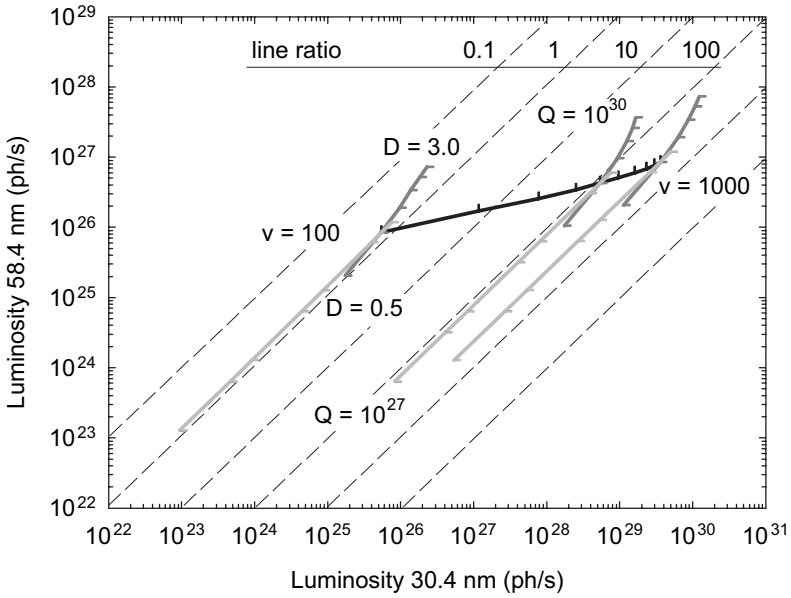

Figure 9.1: *HeI and HeII EUV luminosities of comet Halley. The solid black line indicates the dependence of the helium line emission on the initial velocity of the solar wind (given in units of km s^{-1}). For fixed velocities, the grey lines indicate the influences of changes in gas production (molecules s^{-1}) and heliocentric distance (AU).*

58.4 nm line merely follows the increase of solar wind flux. The ratio between the two helium lines can be seen to be very sensitive to the initial velocity of the solar wind. This behavior is a direct consequence of the strong and weak velocity dependence of the emission cross sections of the 30.4 and 58.4 nm emission, respectively, cf. Figs. 5.6 and 5.7.

The absolute luminosities of the two helium lines depend on the solar wind flux and on cometary characteristics, such as the mass loss rate and the heliocentric distance. Because the largest part of the cometary atmosphere is collisionally thin to charge exchange, the luminosity follows the increase in available neutral donor species. An increase in the mass loss rate or heliocentric distance therefore affects both emission lines in a similar fashion, so that whereas their absolute brightnesses change, the ratio between them is preserved. The ratio between HeII 30.4 nm and HeI 58.4 nm emission can therefore be used to probe the velocity of the wind, whereas absolute line intensities measure a combination of solar wind helium fluxes and comet mass loss rates.

9.1.2 Relative Contributions of Species

In Chapter 5, we presented state selective electron capture cross sections for different species that are abundant in cometary atmospheres. It was demonstrated that below collision velocities of approximately 1000 km s^{-1}, charge exchange cross sections differ per electron donor species.

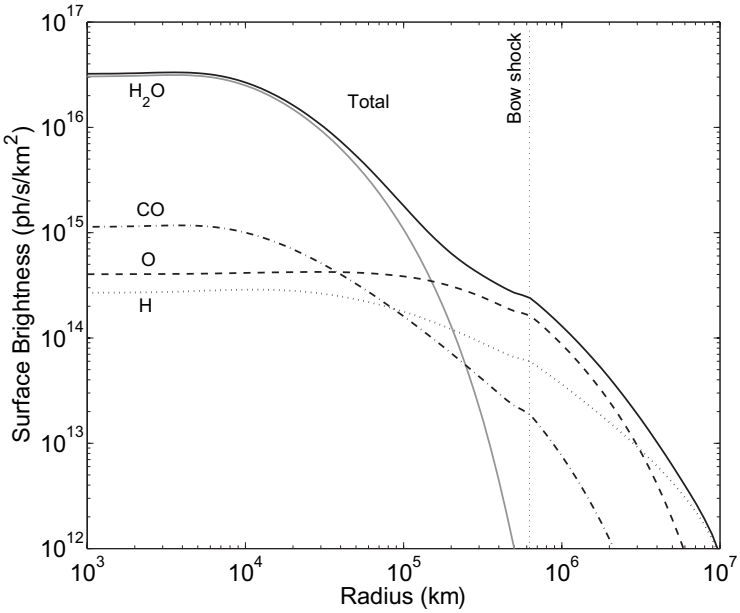

Figure 9.2: *The contribution of neutral cometary species to the surface brightness of the HeII 30.4 nm line within increasing annuli around the nucleus of comet Halley. Black solid line, total; grey solid line, H_2O; dotted line, H: dashed line, O; dash-dotted line, CO.*

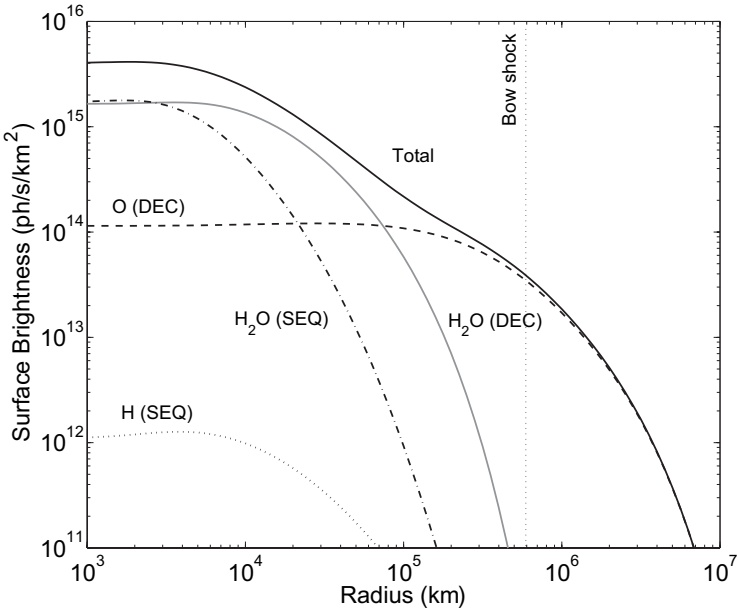

Figure 9.3: *The contribution of neutral cometary species to the surface brightness of the HeI 58.4 nm line within increasing annuli around the nucleus of comet Halley. Black solid line, total; grey solid line, water B2C; dashed-dotted line, water SEQ; dashed line, O B2C; dotted line, atomic H SEQ.*

Figs. 9.2 and 9.3 show which collisions underly the helium line emission of a Halley-like comet-wind interaction. Within ~ 10^5 km from the nucleus, the emission of both lines is dominated by helium colliding on water. Further outward however, the water dissociation products can be seen to take over this role; the HeII 30.4 nm line is then caused by collisions with atomic O and H while the HeI 58.4 nm is due to collisions with atomic O.

Comparing the surface brightness plots with the Haser-model (Fig 8.1), it can be seen that the area where the surface brightness of the 30.4 nm emission is dominated by emission following collisions with water is roughly two times bigger than the region where water molecules are the most abundant neutral species. This difference occurs because emission cross sections for water are much larger than the emission cross sections for O and H (cf. Fig. 5.6). In the case of the HeI 58.4 nm emission, the region where the surface brightness is water-dominated coincides with the region where water is most abundant, as we assumed double electron emission cross sections for collisions with atomic oxygen to be as large as those for collisions with water.

In Fig 9.2, a small kink shows up around 6×10^5 km. This kink is located at the bow shock, which we assumed to be an abrupt transition, and reflects the change of effective collision velocity. Since emission cross sections for double electron capture are roughly constant over the relevant velocity range, the bow shock causes no observable discontinuity in the HeI 58.4 nm emission.

Sequential electron capture plays only a minor role in the deeper lying collisionally thick regions of the comet. The important role of atomic oxygen with regard to the HeI is very interesting, as collisions between He^{2+} and atomic oxygen have barely been studied.

The rate of photo-destruction of cometary neutrals increases with the inverse square of the heliocentric distance r_h. According to the Haser-model, the distance to the nucleus where the number density of water equals the number density of H then depends only on the heliocentric distance with $r_h^{3/2}$. The closer a comet gets to the Sun, the more important emission following charge exchange with water daughter species will become, at the expense of the role of water molecules.

9.1.3 Spatial Effects

The extent of charge exchange emission and the location of its maximum surface brightness depends on the neutral gas distribution in the coma and on the cross sections of the underlying charge exchange processes. Depending on the velocities of the solar wind within the cometary atmosphere, each charge exchange reaction has a specific length scale.

At low densities, charge exchange affects the charge state distribution only marginally. In such collisionally thin environments, EUV and X-ray charge exchange aurorae map the distribution of neutral gas in the coma (cf. the observations of comet 2P/2003 (Encke) by Lisse et al., 2005). When the atmosphere becomes denser and hence collisionally thick to charge exchange, the aurora will take the form of a characteristic 'bowl' (Wegmann et al., 2004), which in projection takes the typical crescent shape observed in the X-ray observations of comet C/1996 B2 (Hyakutake) and C/1999 S4 (Linear) (Lisse et al., 1996, 2001). It is of note here, that total charge exchange cross sections of helium are more than an order of magnitude smaller than total charge exchange cross sections of highly charged solar wind

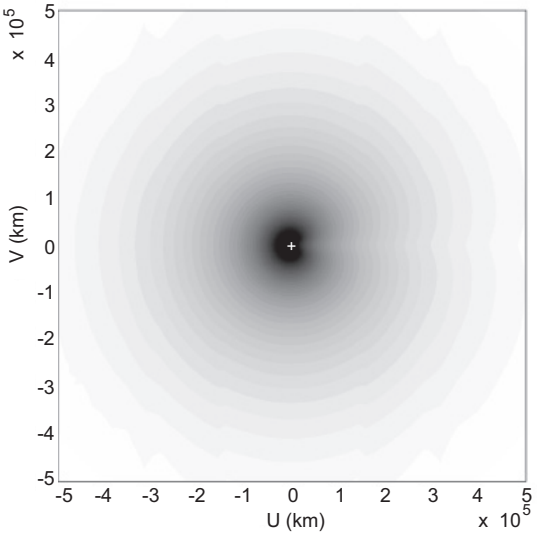

Figure 9.4: *Stretched gray scale image of the morphology of the HeII 30.4 nm emission for a Halley-like comet-wind interaction in arbitrary units, seen with a phase angle of 90°. The comet's nucleus is indicated by a cross hair.. The Sun is to the left.*

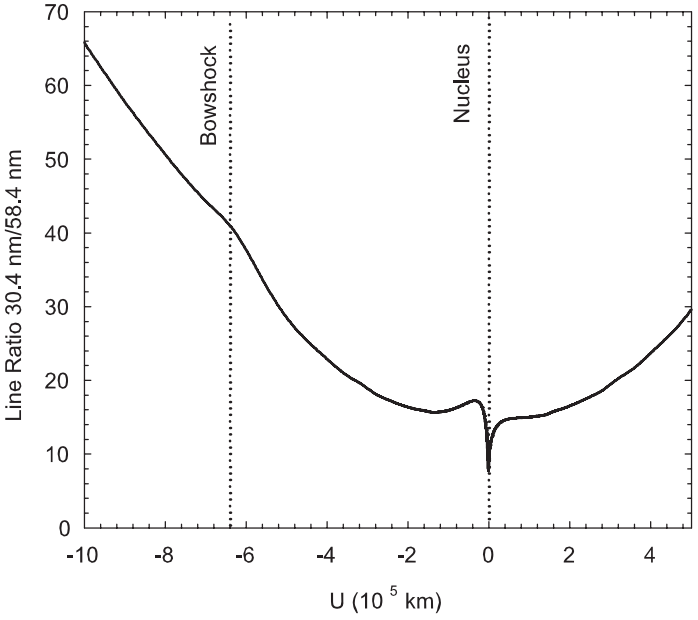

Figure 9.5: *Ratio of the intensities of the HeII 30.4 nm and HeI 58.4 nm emission lines along the comet-Sun axis. The Sun is to the left.*

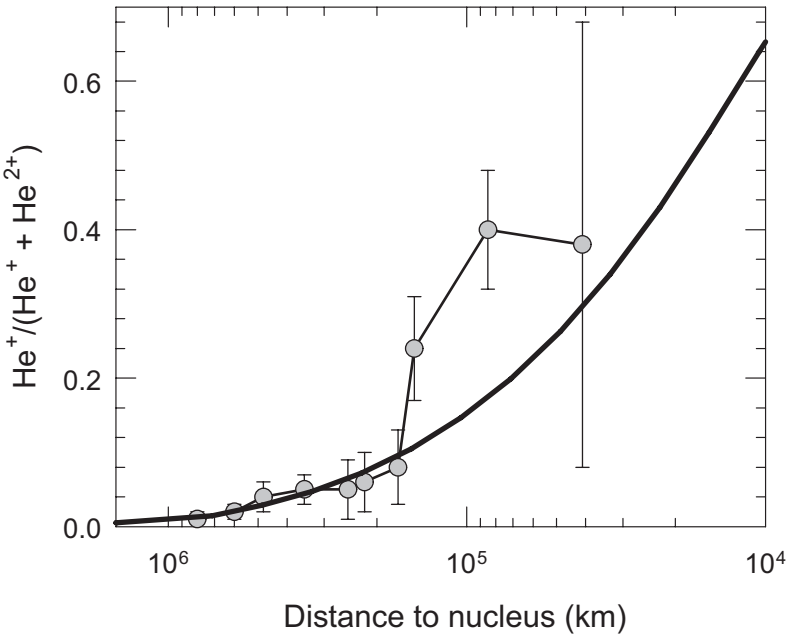

Figure 9.6: *Helium charge state distribution in comet Halley. The solid line represents the predicted distribution. In situ measurements performed by the Giotto probe are indicated by circles.*

oxygen, carbon and nitrogen ions. Different from X-ray observations, EUV emission will therefore display a weaker crescent shape, which is surrounded by a faint symmetric halo from the outer, collisionally thin regions of the coma (see Fig. 9.4).

The spatial behavior of the line emission ratio is illustrated in Fig. 9.5, where the ratio between the HeII 30.4 nm and HeI 58.4 nm line on the comet-Sun axis projected in the observer's plane is shown. Beyond 2×10^5 km of the nucleus, the presence of atomic hydrogen increases the HeII line, thereby increasing the ratio between the HeII and HeI line. The coma is collisionally thick to He^{2+} just before the nucleus, where the ratio increases slightly. The ratio then reaches a minimum, as the He^{2+} state is depleted, and this depletion is also responsible for the shadow behind the nucleus that can be seen in both Fig.s 9.4 and 9.5.

9.2 In Situ Measurements by the *Giotto* Mission

Using experimental total charge exchange cross sections, the charge state distribution was simulated for comet Halley. In situ measurements of both the solar wind velocity (Goldstein et al., 1987) and the helium charge state distribution (Fuselier et al., 1991) performed with the IMS/HERS instruments on board *Giotto* allow for a test of our model. A solar wind velocity of 300 km/s and cometary characteristics as summarized in Table 1 were used. As can be seen from Fig. 9.6, the predicted distribution is in good agreement with the *Giotto*

measurements, up to the magnetic pile-up boundary (1.5×10^5 km, Goldstein et al. (1987)) where complex magneto-hydrodynamics start to govern the interactions.

9.3 Analysis of Existing EUV Observations

Several comets have been observed in the Extreme Ultraviolet (Mumma et al., 1997), and in two cases helium emission has been detected. In comet Hale-Bopp, the 58.4 nm line was observed, but the 30.4 nm was not detected above the background; in comet C/1996 B2 (Hyakutake), it was exactly the other way around as the 30.4 nm line was detected but the 58.4 nm line was not detected above the background. Here, we will apply our model to these comets to demonstrate how cometary EUV emission can be analyzed in terms of charge exchange processes.

9.3.1 C/1996 B2 (Hyakutake)

Comet C/1996 B2 (Hyakutake) was observed with the Extreme Ultraviolet Explorer (EUVE) from March 21 – 25, 1996 (Krasnopolsky et al., 1997). The observing conditions of Hyakutake are summarized in table 9.1. During its observation, the comet was very close to Earth (approximately 0.1 AU) and therefore well studied by different techniques, which help us to reduce the number of free parameters in the model.

A compilation of hourly averages of different solar wind parameters obtained by the WIND and IMP8 spacecraft are available on the internet from the National Space Science Data Center OmniWeb[1]. Following the time shift procedure described by Neugebauer et al. (2000) and using the cometary coordinates summarized in Table 9.1, we find that the wind that interacted with C/1996 B2 (Hyakutake) was monitored on board the spacecrafts between March 21 4:00 UT and March 24 21:00 UT.

The OmniWeb data show a highly variable wind with velocities between 450 and 650 km s^{-1} during the observation and proton densities between 2 – 7 cm^{-3}. Although there

[1] http://nssdc.gsfc.nasa.gov/omniweb/ow.html

Table 9.1: *Observing conditions of C/1996 B2 (Hyakutake). References: 1. Biver et al. (1999); 2. JPL Horizons website*

Parameter	3/21/96	3/25/96	ref.
Q (mol/s)	2×10^{29}		1
Q_{CO} (mol/s)	4×10^{28}		1
R (AU)	1.13	1.05	2
Δ (AU)	0.17	0.10	2
Phase Angle (degrees)	37	58	2
Heliogr. Lat. (degrees)	-3.7	-1.9	2
Heliogr. Long. (degrees)	309	308	2

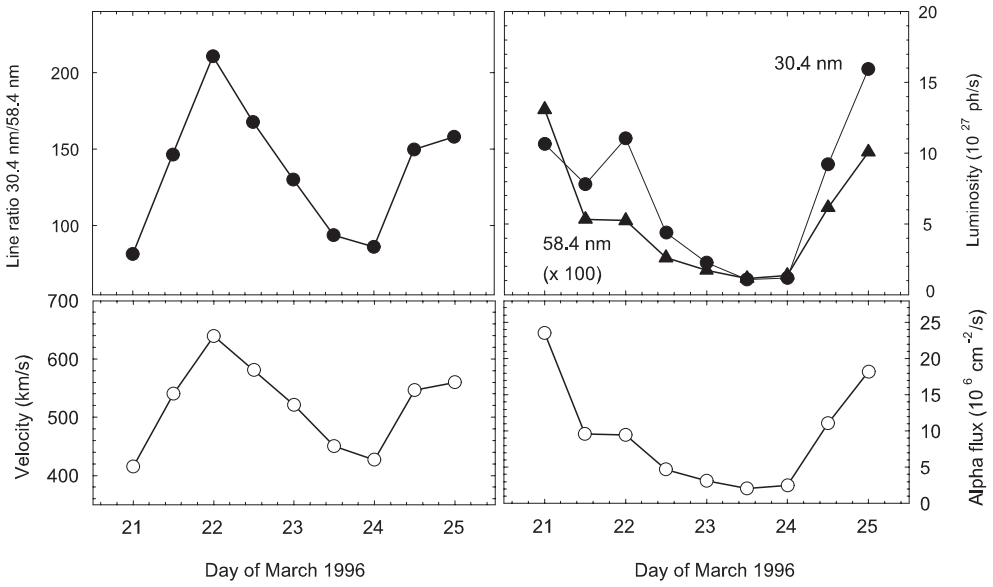

Figure 9.7: *Temporal variability of helium charge exchange emission of C/1996 B2 (Hyakutake) during the* EUVE *observations.* ***Upper left:*** *Calculated ratio of the* HeII *30.4 nm/*HeI *58.4 nm line emission.* ***Upper right:*** *Calculated luminosities of* HeI *58.4 nm and* HeII *30.4 nm.* ***Lower left:*** *Solar wind velocity from OmniWeb as received on C/1996 B2 (Hyakutake)* ***Lower right:*** *Solar wind helium flux from OmniWeb as received on C/1996 B2 (Hyakutake).*

was a 3 – 7° latitudinal separation between comet and spacecraft (Neugebauer et al., 2000) and latitudinal gradients are present in the solar wind, we will use the OmniWeb solar wind data as input parameters to model the EUV emission of comet C/1996 B2 (Hyakutake). The OmniWeb data shows a high variability in solar wind density, velocity and alpha content. This is supported by optical observations of plasma tail disconnection events, which also demonstrate that, during the EUVE observation, comet C/1996 B2 (Hyakutake) interacted with a highly variable (thus equatorial) solar wind (Snow et al., 2004).

Fig. 9.7 shows the predicted total luminosities of the two helium lines during the EUVE observations. Variations in the solar wind helium flux cause the total luminosities of the two helium lines to vary over more than an order of magnitude while the ratio varies with a factor of 2. The 58.4 nm line can be seen to track the alpha particle flux, whereas the behavior of the 30.4 nm line is a convolution of the variation due to the velocity and the flux. The behavior of the line emission ratio therefore directly probes the velocity variations.

The HeII 30.4 nm line was observed to have a photon production rate of 7.3×10^{24} photons/s. The HeI 58.4 nm line was not detected above the background level of 10^{24} photons/s. The two helium lines were observed with two different EUVE detectors; the HeII 30.4 nm line is observed with the medium wavelength spectrometer (MW) while for the HeI 58.4 nm line the long wavelength (LW) spectrometer is required. Due to filter configurations, different apertures were used. The MW and LW detector had apertures of $36.6' \times 9.2'$

Table 9.2: *Summary of C/1996 B2 (Hyakutake) model results and data reduction*

	$L_{30.4}$ (ph/s)	$L_{58.4}$ (ph/s)	ratio
Observation	6.6×10^{24}	$<8\times10^{23}$	$\gtrsim 8$
Model emission in MW aperture	1.48×10^{26}	5.65×10^{24}	26
Model emission in LW aperture	1.35×10^{26}	5.19×10^{24}	26
Model emission after background subtraction (MW aperture)	7.2×10^{24}	(1.6×10^{23})	(45)
Model emission after background subtraction (LW aperture)	(3.9×10^{25})	1.7×10^{24}	(22)
Model results	7.2×10^{24}	1.7×10^{24}	4

and $32.9' \times 9.2'$, respectively, and were both centered on the comet's nucleus. Krasnopolsky et al. (1997) used factors of 1.1 and 1.2 to correct for the different apertures of the MW and LW detector, respectively, so that from the reported values above we deduce photon production rates of 6.6×10^{24} photons/s for the HeII 30.4 nm line and an upper limit of 8.3×10^{23} photons/s for the HeI 58.4 line in the apertures.

As the comet filled the entire field of view, the observers subtracted a tail ward part of the signal from that of a sunward part, based on the assumptions that C/1996 B2 (Hyakutake) was collisionally thick to charge exchange and that its charge exchange emission was homogenous over the observed part of the comet. From our results in section 9.1.3, we expect that for the case of comet Hyakutake, these assumptions are not fully justified. To illustrate this, we summarize the model results, integrated over the time of the observations to take the variability of the wind into account and follow the data reduction procedure of the observers in Table 9.2.

From this table, it can be seen that the different MW and LW aperture sizes do not affect the line ratio and that the emission can be scaled by a factor that accounts for the different aperture sizes. Following the background subtraction procedure of the observers, we calculate luminosities of 7.2×10^{24} and 1.7×10^{24} photons/s for the HeII 30.4 nm and HeI 58.4 nm lines, respectively. We conclude that as much as 90% of the cometary HeII emission line and 65% of the HeI emission was subtracted as 'background'.

Given the uncertainties introduced by the background subtraction procedure of the observation, the uncertainties in the initial solar wind conditions, and the high variability of the solar wind during the observations, the model reproduces the observations very well.

The case of comet C/1996 B2 (Hyakutake) shows both the observational difficulties and potential diagnostic richness of cometary charge exchange aurorae. The temporal behavior of relative and absolute line emission can be used to remotely study solar wind characteristics whereas their spatial distribution provides access to the interaction between the comet and the wind.

Table 9.3: *Observing conditions of C/1995 O1 (Hale-Bopp). References: 1. Biver et al. (1999); 2. JPL Horizons website*

Parameter	9/14/96	9/20/96	ref.
Q (molec./s)	6×10^{29}		1
Q_{CO} (molec./s)	2×10^{29}		1
Q_{CO_2} (molec./s)	6×10^{28}		1
R (AU)	3.09	3.03	2
Δ (AU)	2.90	2.92	2
Phase Angle (degrees) .	19	19	2
Heliogr. Lat. (degrees) .	19	20	2
Heliogr. Long. (degrees)	44	44	2

9.3.2 C/1995 O1 (Hale-Bopp)

Comet C/1995 O1 (Hale-Bopp) was observed with the EUVE observatory from September 14-19, 1996 by Krasnopolsky et al. (1997). The observing conditions of Hale-Bopp are summarized in Table 9.3.

An estimate of the solar wind conditions at Comet C/1995 O1 (Hale-Bopp) during the EUVE observations is obtained by mapping measurements made in-situ by the *Ulysses* spacecraft to the comet's position. The *Ulysses* data over the period of interest are summarized in Fig. 9.8. At the time, *Ulysses* was at a solar latitude of 26 degrees North, while C/1995 O1 (Hale-Bopp) was at 19.9 degrees North. The spacecraft was separated from C/1995 O1 (Hale-Bopp) by around 130° in longitude; Hale-Bopp was at a heliocentric distance of 3.05 AU, while *Ulysses* was at 4.35 AU. Solar wind conditions might have varied between the spacecraft and the comet, but as the structure of the solar wind around this time was fairly stable, and the parameters observed by *Ulysses* were fairly constant from one rotation to the next, it seems justifiable to use the solar wind conditions observed by *Ulysses* and summarized in Table 9.3 as initial conditions in our model.

From the *Ulysses* data, C/1995 O1 (Hale-Bopp) would have interacted with a quiet, fast solar wind. There is some variability in the alpha-particle measurements, that differs from that seen in the protons. As is illustrated in Fig. 9.8, we predict that during the observations, the ratio between the HeII and HeI emission was constant, whereas the absolute intensities closely followed the solar wind helium flux and varied less than a factor of 3.

Krasnopolsky et al. (1997) observed a photon production rate of 1.2×10^{26} photons/s for the HeI 58.4 nm emission line within a projected slit of $5.4 \times 10^5 \times 3.6 \times 10^5$ km^2. Within this slit, the HeII was not detected above a 2σ upper limit of 7×10^{25} photons/s. Neither line was detected in the subtracted background spectrum, to a level of $\lesssim 3\%$ of the background continuum emission. Our model predicts that within this slit, the helium lines drop to less than 15% of the average surface brightness of the coma, and would 'disappear' into the background.

Averaging the results shown in Fig. 9.8 over the time of the observations, we find total photon production rates of 7.6×10^{26} and 2.9×10^{25} photons/s for the HeII 30.4 nm and

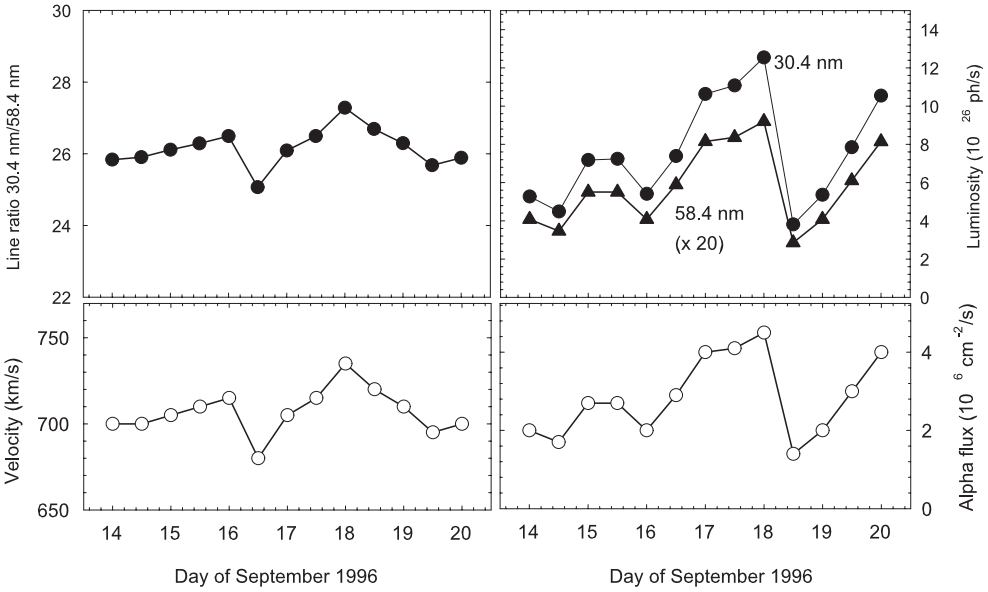

Figure 9.8: *Temporal variability of helium charge exchange emission of C/1995 O1 (Hale-Bopp) during the EUVE observations.* ***Upper left:*** *Calculated ratio between the HeII 30.4 nm and HeI 58.4 nm line emission.* ***Upper right:*** *Calculated luminosities of HeI 58.4 nm and HeII 30.4 nm.* ***Lower left:*** *Solar wind velocity from Ulysses as received on C/1995 O1 (Hale-Bopp).* ***Lower right:*** *Solar wind helium flux from Ulysses as received on C/1995 O1 (Hale-Bopp).*

the HeI 58.4 nm lines, respectively. Our model thus overestimates the HeII emission by a factor of 10 and underestimates the HeI emission within a factor of 4. We know of no other processes that can efficiently contribute to the HeI emission (Bodewits et al., 2004). Following Fig. 9.1, this suggests that comet C/1995 O1 (Hale-Bopp) interacted with a higher alpha particles flux, via either the total solar wind flux or the alpha particle abundance in the solar wind (hence increasing the luminosities of both helium emission lines) and also much slower (hence decreasing the HeII 30.4 nm emission but preserving the HeI 58.4 nm emission).

There are two different possible scenarios to fit the model to the observation, but we cannot distinguish between them as only total photon production rates are available.

Table 9.4: *Summary of C/1995 O1 (Hale-Bopp) observational and model results.*

	$L_{30.4}$ (ph/s)	$L_{58.4}$ (ph/s)	ratio
Observation	$< 7 \times 10^{25}$	1.2×10^{26}	$\gtrsim$0.6
Model results	7.6×10^{26}	2.9×10^{25}	26

First, the comet could have interacted with a slower, denser wind. According to our model, this would require an initial wind velocity below 200 km s^{-1} and an unrealistically high helium flux of 5×10^7 cm^{-2}/s, 17 times more than the flux observed by Ulysses.

It is possible that, although mapped *Ulysses* data suggest that Hale-Bopp was in fast, polar coronal hole solar wind at the time of observation, the lower heliolatitude of the comet compared to the spacecraft meant that it may actually have been south of the northern boundary of the streamer belt. Such a situation would yield a lower solar wind velocity, and higher solar wind particle number density at Hale-Bopp, with both of these parameters being more variable than in the fast, coronal hole flow. *Ulysses* and ground-based observations suggest that the heliospheric current sheet did extend to as high as 30 degrees north heliolatitude at the time (Forsyth et al., 1997). Ultimately, the solar wind conditions at Hale-Bopp at the time will not be determined absolutely, but even if the comet was within the streamer belt, it is unlikely that the velocity would be as low as 200 km s^{-1}, as required by our model.

Alternatively, the difference between modeled and observed HeII photo production rates might be explained in terms of cooling and slow down of the solar wind within the coma. At 3 AU from the Sun, C/1995 O1 (Hale-Bopp) was already an exceptionally large comet with a huge ionopause distance. According to Eq. 8.4, the bow shock must have been over 10^7 km from the nucleus; in contrast, for comet C/1996 B2 (Hyakutake), the bow shock was located at only a few 10^5 km in front of the nucleus. Our model can explain the observation in this scenario if the solar wind, with an initial velocity of 700 km s^{-1}, would have been cooled and slowed down to a mean collision velocity of $\lesssim$ 175 km s^{-1} in the interaction zone. To explain the observed luminosities, an alpha flux of 1.5×10^7 $cm^{-2}s^{-1}$ is needed, which is 5 times higher than the wind sampled by Ulysses. It would be most interesting to test these hypotheses with magnetohydrodynamic comet-wind models.

9.4 Summary and Conclusions

Within the limitations of available EUV observations of comets, we have illustrated the manifold consequences of the charge exchange interaction process. Clear spectral, temporal and morphological effects should be detectable for different comet – solar wind conditions. The main findings of this work are the following:

1. Emission cross sections are very sensitive to velocity effects. Every charge exchange reaction has its own particular behavior with respect to the velocity, so that line emission ratios - in our case the ratio between the HeII 30.4 nm and the HeI 58.4 nm line - can be used for velocimetry. Absolute intensities can be used to determine local heavy ion fluxes.

2. Different electron capture cross sections imply different emission length scales. Spatial gradients in charge exchange line emission ratios hence contain a wealth of information on the interaction between comet and solar wind. This also implies, that it will be very difficult to interpret spectra that are produced by integration over the full projected image of the comet as in the cases of the two comets discussed.

3. Water and its dissociation products O and H are the most important collision partners for charge exchange reactions in cometary atmospheres. Our model predicts that atomic oxygen is the most important multi-electron donor in the outer regions of the comet, but experimental data on charge exchange reactions is lacking.

4. Emission following double electron capture is the most important source of cometary EUV emission next to single electron capture. Sequential capture contributes only marginally to the HeI 58.4 nm emission. Interestingly, multiple electron capture has not been included in simulations of cometary X-ray spectra (cf. Ali et al. (2005)).

We have applied our model to the observation of helium emission in the comets C/1996 B2 (Hyakutake) and C/1995 O1 (Hale-Bopp). For Hyakutake, the comparison between model and observation is severely hampered by the large background correction. Nevertheless, our model seems to reproduce the observations well. The model results illustrate that the time variability of the different lines might provide a powerful tool as interaction diagnostics.

The case of C/1995 O1 (Hale-Bopp) illustrates well the dependence of the helium line emission to the collision velocity. For Hale-Bopp, our model requires low velocities in the interaction zone. We interpret this as the effect of severe post bow shock cooling in this extraordinary large comet.